Since January 2020 Elsevier has created a COVID-19 resource centre with free information in English and Mandarin on the novel coronavirus COVID-19. The COVID-19 resource centre is hosted on Elsevier Connect, the company's public news and information website.

Virus Research 280 (2020) 197901

Contents lists available at ScienceDirect

Virus Research

journal homepage: www.elsevier.com/locate/virusres

Decreased NHE3 activity and trafficking in TGEV-infected IPEC-J2 cells via the SGLT1-mediated P38 MAPK/AKt2 pathway

Yang Yang[1], Qiuhan Yu[1], Han Song[1], Ling Ran, Kai Wang, Luyi Xie, Shilei Huang, Zheng Niu, Yilin Zhang, Zifei Kan, Tao Yan, Zhenhui Song*

Department of Veterinary Medicine Southwest University Chongqing People's Republic of China, Chongqing 402460, China

ARTICLE INFO

Keywords:
Transmissible gastroenteritis virus
Sodium/hydrogen exchanger 3
Sodium glucose cotransporters 1
Translocation

ABSTRACT

Transmissible gastroenteritis virus (TGEV) primarily replicates in intestinal epithelial cells and causes severe damage to host cells, resulting in diarrhea. Surface NHE3 serves as the key regulatory site controlling electroneutral Na^+ absorption. In this study, our results showed that the surface NHE3 content was significantly reduced following TGEV infection, whereas the total level of protein expression was not significantly changed, and NHE3 activity gradually decreased with prolonged infection time. We then inhibited SGLT1 expression by lentiviral interference and drug inhibition, respectively. Inhibition studies showed that the level of phosphorylation of the downstream key proteins, MAPKAPK-2 and EZRIN, in the SGLT1-mediated p38MAPK/AKt2 signaling pathway was significantly increased. The surface NHE3 expression was also significantly increased, and NHE3 activity was also significantly enhanced. These results demonstrate that a TGEV infection can inhibit NHE3 translocation and attenuates sodium-hydrogen exchange activity via the SGLT1-mediated p38MAPK/AKt2 signaling pathway, affecting cellular electrolyte absorption leading to diarrhea.

1. Introduction

Diarrhea caused by coronaviruses is a key contributor to the morbidity and mortality of piglets throughout the world, primarily in suckling and weaned piglets (Katsuda et al., 2006; Butler et al., 1974). Transmissible gastroenteritis virus (TGEV) is a coronavirus characterized by severe diarrhea, vomiting, and dehydration, with the death rates as high as 100 % in one-week-old piglets, whereas three-week-old infected piglets survive; however, these recovered piglets can spread TGEV to other uninfected piglets for several days (Tajima, 1970; Leopoldt and Meyer, 1978; Lawhorn, 2007). Moreover, TGEV has been reported to cause a severe infection in mature mucosal epithelial cells of the proximal small intestine, induce villi atrophy, and reduce the villous height and crypt depth (Xia et al., 2018). In addition, BuTRr has also been found in the diarrhea of piglets infected with TGEV, and exhibited increased quantities and concentrations of sodium, potassium, and chloride in the stools (Kelly et al., 1972).

Diarrhea is closely related to the activity and expression of ion transporters expressed on the surface of intestinal epithelial cells. Under normal physiological conditions, the balance of absorption and secretion of intestinal water and electrolytes plays an important role in maintaining homeostasis of the intestinal environment (Field, 2003; Zhang et al., 2012). Although viruses, bacteria, and some enterotoxins invade intestinal epithelial cells, the expression and activity of related ion channels and transport carriers on intestinal epithelial cells undergo abnormal changes, leading to disturbances in the absorption and secretion of water and electrolytes (i.e., Na^+). Na^+/H^+ exchanger 3 (NHE3), belongs to the SLC9A family and is present in the intestinal and renal epithelia, which is primarily responsible for the electrical neutral absorption of Na^+ (Dynia et al., 2010). Moreover, *Nhe3*$^{-/-}$ mice have an absorptive defect in the intestine and kidney, and suffer from an acid-base unbalance and Na^+-fluid volume disorder (Schultheis et al., 1998).

The acute regulation of NHE3 activity is primarily focused on the circulation of NHE3 between the plasma membrane and intracellular compartment, and there is evidence to suggest that the up-regulation of NHE3 activity can be mediated by the rapid insertion of NHE3 into the plasma membrane from within the cell (D'Souza et al., 1998; Janecki, 2000). Na^+-glucose co-transporter1 (SGLT1) is predominantly expressed in the mucosa of the small intestine and has been found to play an important role in the absorption of Na^+ and glucose (Xu et al., 2018; Wright et al., 2004). Previous studies have demonstrated that SGLT1

* Corresponding author.
E-mail address: szh7678@126.com (Z. Song).
[1] Yang Yang, Qiuhan and Han S contributed equally to this work.

https://doi.org/10.1016/j.virusres.2020.197901
Received 19 September 2019; Received in revised form 9 January 2020; Accepted 14 February 2020
Available online 15 February 2020
0168-1702/

can regulate NHE3 translocation to the plasma membrane via the p38MAPK/Akt2 signaling pathway in intestinal epithelial cells via the sequential activation p38 mitogen-activated protein kinase (MAPK), MAPK-activated protein kinase 2 (MAPKAPK-2), Akt2, and ezrin (Cha and Donowitz, 2008); however, the role of SGLT1-induced NHE3 translocation in viral infection remains unknown.

Therefore, in the present study, we aimed to demonstrate the effects of TGEV infection on NHE3 translocation and the associated molecular mechanisms. Our data demonstrate that TGEV can reduce the level of NHE3 protein expression on the cell membrane and NHE3 activity via the SGLT1-mediated p38MAPK/AKt2 signaling pathway.

2. Materials and methods

2.1. Cells and viruses

Porcine jejunum intestinal cells (IPEC-J2) were purchased from Shanghai Zishi Biotechnology, grown in Roswell Park Memorial Institute (RPMI) 1640 medium (Gibco, United States) supplemented with 10 % fetal bovine serum (FBS, Gibco), and maintained in maintenance medium (RPMI 1640 supplemented with 2% FBS) in a 5% CO_2 incubator. The TGEV Miller strain was preserved in our laboratory.

2.2. Lentivirus-mediated RNA interference

The lentiviral vector, piLenti-siRNA-GFP, was constructed to express short hairpin RNA for RNAi studies by the Rhonin Biosciences Company (China). The four siRNAs were designated as, siRNA a, siRNA b, siRNA c, and siRNA d, respectively. The optimal multiplicity of infection based on the results of the lentivirus titer given by the manufacturer was explored, and the lentiviral particles (MOI = 5) were added to the IPEC-J2 cells and screened for the stable expression of the siRNA cell line.

2.3. Inhibitor

Phlorizin (MCE, China) was selected as an SGLT1 inhibitor and an MTT assay was used to evaluate the maximum concentration that resulted in a 50 % cell survival inhibition rate.

2.4. Western blot

IPEC-J2 cells were washed three times with cold-PBS and lysed in radioimmunoprecipitation assay (RIPA, 200 μL/well) buffer (Beyotime, China) containing protease inhibitors (PMSF, 100 mM). The protein concentration of the resulting lysates was determined using a Pierce BCA (Beyotime, China). After centrifugation at 11,000 × g for 15 min, the proteins in the supernatant (40 μg protein) were separated by sodium dodecyl sulfate polyacrylamide gel electrophoresis (SDS-PAGE) on 12 % gradient gels, and transferred to polyvinylidene fluoride (PVDF) membranes (Merck Millipore, Darmstadt, Germany). The membranes were blocked for 1 h in Tris-buffered saline (TBS) containing 5 % non-fat dry milk at room temperature (phosphorylated proteins were blocked in 5 % BSA), and incubated with the primary antibodies at 4 °C overnight. After washing three times with TBST, the membranes were incubated with HRP-conjugated goat anti-rabbit IgG (Sangon Biotech) at 37 °C for 1 h. The proteins were visualized using 3,3′-diaminobenzidine, and detected by enhanced chemiluminescence (ECL; Thermo Scientific) and autoradiography.

2.5. RT-qPCR

The total RNA was extracted using RNAiso plus (Invitrogen, USA) reagent and subjected to reverse transcription with 5× PrimeScript RT Master Mix (Promega, USA). A quantitative real-time PCR (qPCR) analysis was performed to amplify the SGLT1 and NHE3 genes using the cDNA as the template and the β-actin gene as an internal standard. The qPCR reaction contained 10 μL of SYBR Premix ExTaq II (Takara Bio, China), 0.5 μL forward primer, 0.5 μL reverse primer, 1 μL of cDNA template, and RNase-free ddH_2O was added to 20 μL. The reaction protocol was as follows: 95 °C for 30 s, followed by 40 cycles of 95 °C for 5 s, and 60 °C for 30 s; each sample was repeated three times. These primers are presented in Table 1. Data analysis was based on the measurement of the cycle threshold (Ct). The relative level of SGLT1 and NHE3 mRNA expression were calculated using the $2^{-\triangle\triangle Ct}$ method.

2.6. IFA analyses

Cell climbing slices (Solarbio, YA0350, CN) were placed at the bottom of 24-well and before seeding IPEC-J2 cells. TGEV infected group, control group, siRNA groups and Phlorizin group were set up, 3 repeat well for each group. The slices were washed by PBS thrice for 5 min each time, followed by fixing in 4 % paraformaldehyde for 30 min. The slices were again washed with PBS thrice for 5 min each time, they were blocked with 5 % BSA for 60 min, followed by PBS washes thrice for 3 min each and incubated with the primary antibodies in a wet dish at 4 °C overnight. Washing with PBS thrice for 3 min each time. Then incubation with Anti-rabbit IgG (H + L) F(ab')2 Fragment (Alexa Fluor® 594 Conjugate) antibody (Cell Signaling Technology) and Anti-Rabbit IgG (whole molecule)–FITC antibody (Sigma-Aldrich) for 30 min, washing three times. Staining was performed using DAPI (Beyotime, CN) for 5 min, followed by PBS washed thrice for 5 min each, add 3–5 drops of antifade mounting medium (Beyotime, CN). The samples were visualized by laser confocal microscopy (Axio-Imager LSM-800, Carl Zeiss AG).

2.7. Determination of the intracellular and extracellular sodium ion concentration

The intracellular and extracellular sodium ion concentration was detected using Flame Atomic Absorption Spectrometry as previously described (Yang et al., 2018). IPEC-J2 cells were infected with TGEV after transfection with siRNA b and lysed in a radioimmunoprecipitation assay (RIPA) solution as an intracellular sodium ion sample, and the extracellular samples were collected from the cell culture supernatant. A Na^+ standard solution (10 mg/mL) was prepared by dissolving 1 mL of the Na^+ standard solution 1000 mg/mL in 100 mL of deionized water, then diluted into standard working solutions dissolving 2.593 g of KNO_3 in 50 mL of 5 % HNO_3, and then diluted to 500 mL with deionized water) of 0.05, 0.1, 0.2, and 0.4 mg/mL. The samples were diluted by 5 × 10^3-fold and detected by the TAS-990 atomic absorption spectrometer at the following condition: wavelength of 589 nm, negative high-voltage of 297 V, current of 2 mA, and a gas flow of 1200 mL min^{-1}.

2.8. Measurement of the Na^+/H^+ exchange activity

The level of NHE3 activity in IPEC-J2 cells was measured fluorometrically using the pH sensitive dye, BCECF-AM, as previously described (Murtazina et al., 2006). Briefly, the cells were grown on a 96-well cell culture plate and loaded with 5 μM BCECF-AM for 30 min at 37 °C. The cells were then washed with an Na^+-solution (138 mM NaCl; 5 mM KCl; 2 mM $CaCl_2$; 1 mM $MgSO_4$; 1 mM NaH_2PO_4; 25 mM glucose; and 20 mM HEPES, pH 7.4) to remove any extracellular dye. The baseline pHi was measured using a fluorescent multi-function microplate reader (Teacan, Switzerland) and the ratio of fluorescence was estimated (λ-excitation: 440 nm and 490 nm; λ-emission: 530 nm). The cells were exposed to 40 mM $NHCl_4$ (pH 7.4) which caused alkalization, and the cells were perfused with an Na^+-free solution (130 mM tetramethylammonium (TMA) chloride, 5 mM KCl, 2 mM $CaCl_2$, 1 mM $MgSO_4$, 1 mM NaH_2PO_4, 25 mM glucose, and 20 mM HEPES, pH 7.4),

resulting in cellular acidification. Finally, the re-addition of the Na^+-solution (138 mM NaCl, 5 mM KCl, 2 mM $CaCl_2$, 1 mM $MgSO_4$, 1 mM NaH_2PO_4, 25 mM glucose, and 20 mM HEPES, pH 7.4) and measurement of the pH at the end of each experiment, the fluorescence ratio was calibrated to the appropriate pH using nigericin (2 μM; Sigma-Alrich)/high K^+ solutions at different pH values. NHE3 activity was measured by calculating the change in pH over the first 1 min and expressed as ΔpH/min.

2.9. Measurement of surface NHE3 expression

The surface expression of NHE3 in IPEC-J2 cells was determined separately by cell-surface biotinylation as previously described (Murtazina et al., 2006). Briefly, the cells were washed with cold-PBS (150 mM NaCl and 20 mM Na_2HPO_4, pH 7.4), resuspended in PBS, incubated with 1 mg/mL Sulfo-NHS-SS-Biotin (APExBIO, USA) for 30 min at room temperature, and washed with quenching buffer containing 15 mM Glycine to scavenge the unbound biotin. The cell sedimentation was lysed in RIPA buffer (Beyotime, China) containing 100 mM protease inhibitor on ice for 1 h, and the lysates were centrifuged at 11,000 × g for 15 min to remove any excess biotin reagent and byproducts. The protein concentration in the supernatants was determined using a Pierce BCA (Beyotime, China), and partial supernatants were used for an analysis of the total protein content. The amount of streptavidin agarose was calculated with protein concentrations (1 mL streptavidin agarose can bind 6 mg protein) and reacted for 90 min at 4 °C. The samples were then washed three times with RIPA containing 100 mM protease inhibitor and centrifuged at 500 × g for 30 s to remove the unbound protein. Next, 6× protein loading buffer was added and denatured at 100 °C for 5 min. A Western blot was used to analyze the percentage of the total level of cellular NHE3 expression at the apical surface of IPEC-J2 cells.

2.10. Statistics

All statistical calculations were performed using GraphPad Prism 7.0. All data are presented as the mean ± SD or with the standard errors of the mean from three independent experiments. A one-way analysis of variance (ANOVA) and *t*-test were employed to determine the statistical differences between multiple groups. P-values less than 0.05 were considered statistically significant (*P-value < 0.05; **P-value < 0.01; *** P-value < 0.001).

3. Results

3.1. TGEV infection is related to the expression of surface NHE3 and the activity of Na^+/H^+ exchange

It has been well-established that NHE3 expression on the surface of small intestinal epithelial cells is primarily responsible for the neutral exchange of sodium ions; however, whether TGEV infection is related to the level of NHE3 protein expression on the cell surface remains unclear (Brett, 2005; Chow et al., 1999). As shown in (Fig. 1A —E), TGEV infection was found to significantly reduce the level of surface NHE3 protein expression and suppress sodium hydrogen exchange at 72 h-post infection (hpi) by WB and IFA analysis. However, there was no significant change in the level of total NHE3 protein expression. The level of total NHE3 mRNA expression was significantly decreased at 24 h-post infection, and tends to increase gradually with the length of infection (Fig. 1F). These data suggest that TGEV infection can suppress NHE3 activity by decreasing the level of surface NHE3 protein expression.

We also examined the effect of TGEV infection on SGLT1 expression and the infection efficiency of TGEV. The results of Fig. 2A — B displayed a higher level of SGLT1 expression than that of the control group at 48 h-post infection. The level of mRNA expression was not significantly changed at 24 hpi, but exhibited a gradual increasing trend as the length of viral infection progressed (Fig. 2C), Fig. 2D-E showed TGEV infection efficiency in IPEC-J2 at 24 h, 48 h and 72 h.

3.2. Regulation of SGLT1 on NHE3 translocation in mock-infected cells

Some studies have shown that together, SGLT1 and NHE3 regulate sodium absorption in epithelial cells (Coon et al., 2011); however, it is unclear what a physiological relationship between SGLT1-medated activation of the p38MAPK/Akt2 pathway and regulation of NHE3 translocation. To explore the associated regulatory relationships, we inhibited SGLT1 expression by transfection with siRNAs and treatment with inhibitors.

Firstly, the IPEC-J2 cells were transfected with four lentiviral-mediated SGLT1-specific siRNAs to filter out the interference with an efficient siRNA plasmid. The results showed that siRNA b could markedly down-regulate the level of SGLT1 protein and mRNA expression compared with other groups (Fig. 3A — C). Then IPEC-J2 cells transfected with the siRNA b were assessed for changes in the expression of key proteins and surface NHE3 content by Western blot and IFA. As shown in Fig. 3D —H, compared with the control group, silencing of SGLT1 using siRNA b can significantly up-regulate the expression of p-MAPKAPK-2 and p-EZRIN, as well as the NHE3 expression on the plasma membrane. and the results were further verified by the IFA analysis, as shown in the Fig3I-J, the fluorescence expression of surface NHE3 in siRNA b-treated group was significantly stronger than that in the control group. Notably, there was no significant change in the sodium ion concentration inside and outside the cell following transfection with siRNA b compared with the control group (Fig.3K).

Furthermore, Phlorizin was selected as an SGLT1 inhibitor, and we used a 3-(4,5-dimethylthiazol-2-yl)-2,5-diphenyltetrazolium bromide (MTT) assay to assess the level of cytotoxicity. The results showed When phlorizin reached concentrations as 200 μM, more than 50 % of IPEC-J2 cells remained viable that means it's IC50 was 200 uM (Fig. 4A), so 200 μM was the optimal toxic dosage of Phlorizin in IPEC-J2 cells. Cells treated with 200 μM Phlorizin displayed an up-regulation of p-MAPKAPK-2 and p-EZRIN expression (Fig. 4D-K). Increased NHE3 protein content on the cytoplasmic membrane (Fig. 4B,C,D and J) was also observed, which in turn, led to enhanced activity of NHE3 (Fig. 4L). In conclusion, these results suggest that the inhibition of SGLT1 by siRNA or Phlorizin treatment promote NHE3 translocation via the p38MAPK/Akt2 pathway, and resulted in increased NHE3 activity.

3.3. Inhibition of SGLT1 promotes the translocation of NHE3 in TGEV-infected cells

We have revealed that down-regulated SGLT1 expression could promote the translocation of NHE3 through the p38MAPK/Akt2 pathway. Moreover, TGEV infection led to increased SGLT1 protein expression and decreased cell surface NHE3 protein content as shown in previous studies. Thus, we hypothesize that TGEV infection may regulate NHE3 expression via SGLT1-mediated activation of the p38MAPK/Akt2 signaling pathway.

Firstly, in IPEC-J2 cells transfected with siRNA b and incubated with the virus for 48 h, the expression of key proteins in the p38MAPK/Akt2 signaling pathway was analyzed by Western blot. As shown in the Fig. 5A — E, compared with the TGEV-infected group, a significant down-regulation of SGLT1 expression could up-regulate p-MAKPAKP-2 and p-EZRIN protein expression, as well as increased surface NHE3 protein expression. These results suggest that inhibiting SGLT1 expression can promote NHE3 translocation via the p38MAPK/Akt2 signaling pathway following TGEV infection.

The cells were then treated with 200 μM Phlorizin for 15 min, followed by an incubation with TGEV for 48 h. As shown in Fig. 6A — E, when SGLT1 protein expression was significantly inhibited, there was

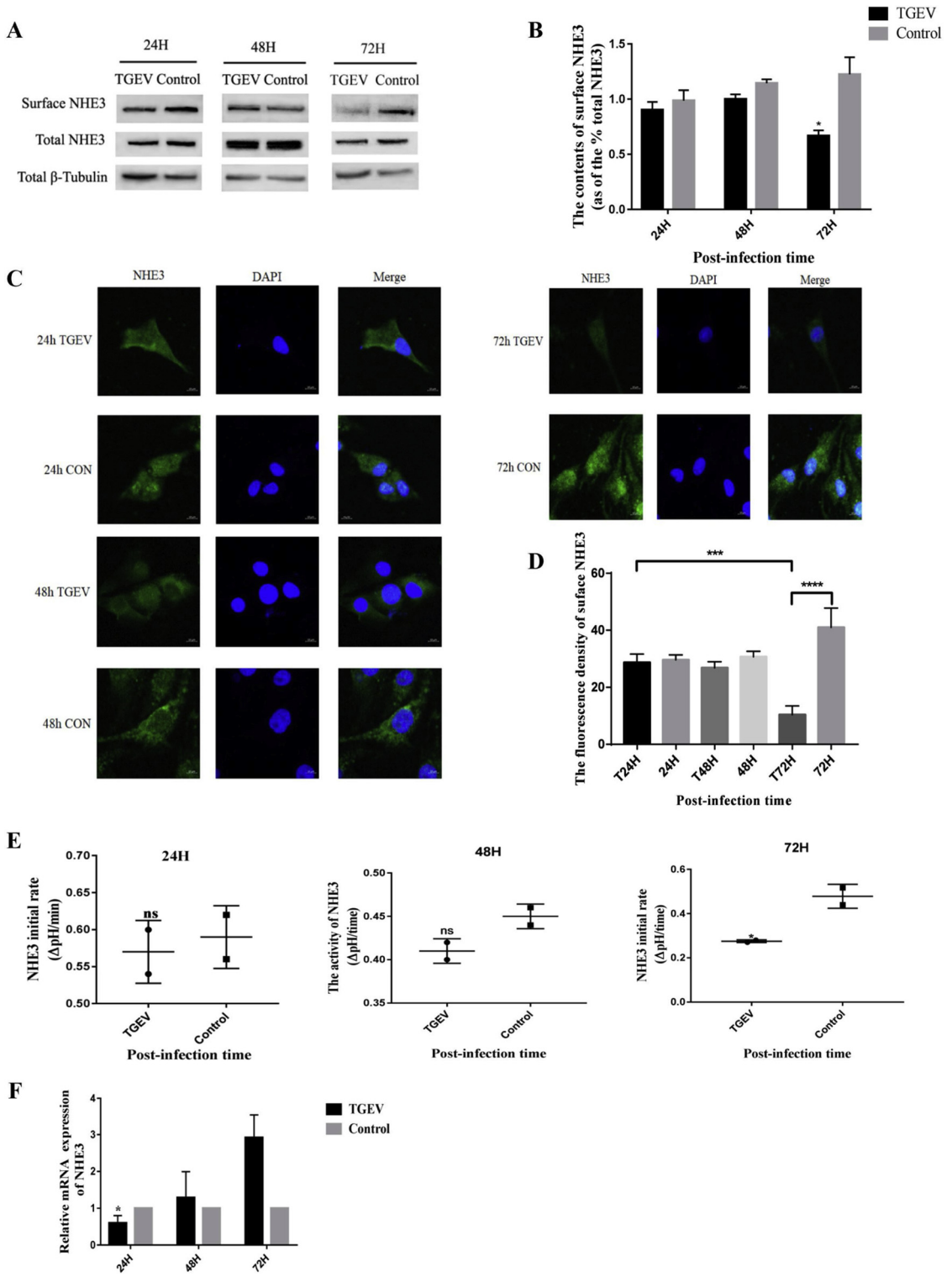

Fig. 1. The effect of TGEV infection on NHE3 activity, the expression of NHE3. (A) IPEC-J2 cells infected TGEV Miller (MOI = 0.1) for 24 h, 48 h, 72 h at 37 °C and then surface-biotinylated as described under "Experimental Procedures". The surface and total of NHE3 protein expression were analyzed by western-blot. (B) Grayscale analysis of the surface NHE3/total NHE3. (C) IPEC-J2 cells infected TGEV Miller (MOI = 0.1) for 24 h, 48 h, 72 h at 37 °C and then immunofluorescence as described under "Experimental Procedures". The surface NHE3 protein expression were analyzed by Image-Pro Plus 6.0. (D) The fluorescence intensity of surface NHE3. (E) NHE3 activity were analyzed by using pH sensitive dye BCECF-AM. (F) The mRNA expression levels of NHE3 were detected using qRT-PCR and normalized by the β-Actin mRNA level.

no significant change in p-MAPKAPK-2 expression, whereas p-ZERIN protein expression was markedly up-regulated, and the surface NHE3 protein content continued to increase. These results indicate that the inhibition of SGLT1 expression could promote NHE3 translocation via the EZRIN-mediated pathway but may be independent of MAPKAPK-2.

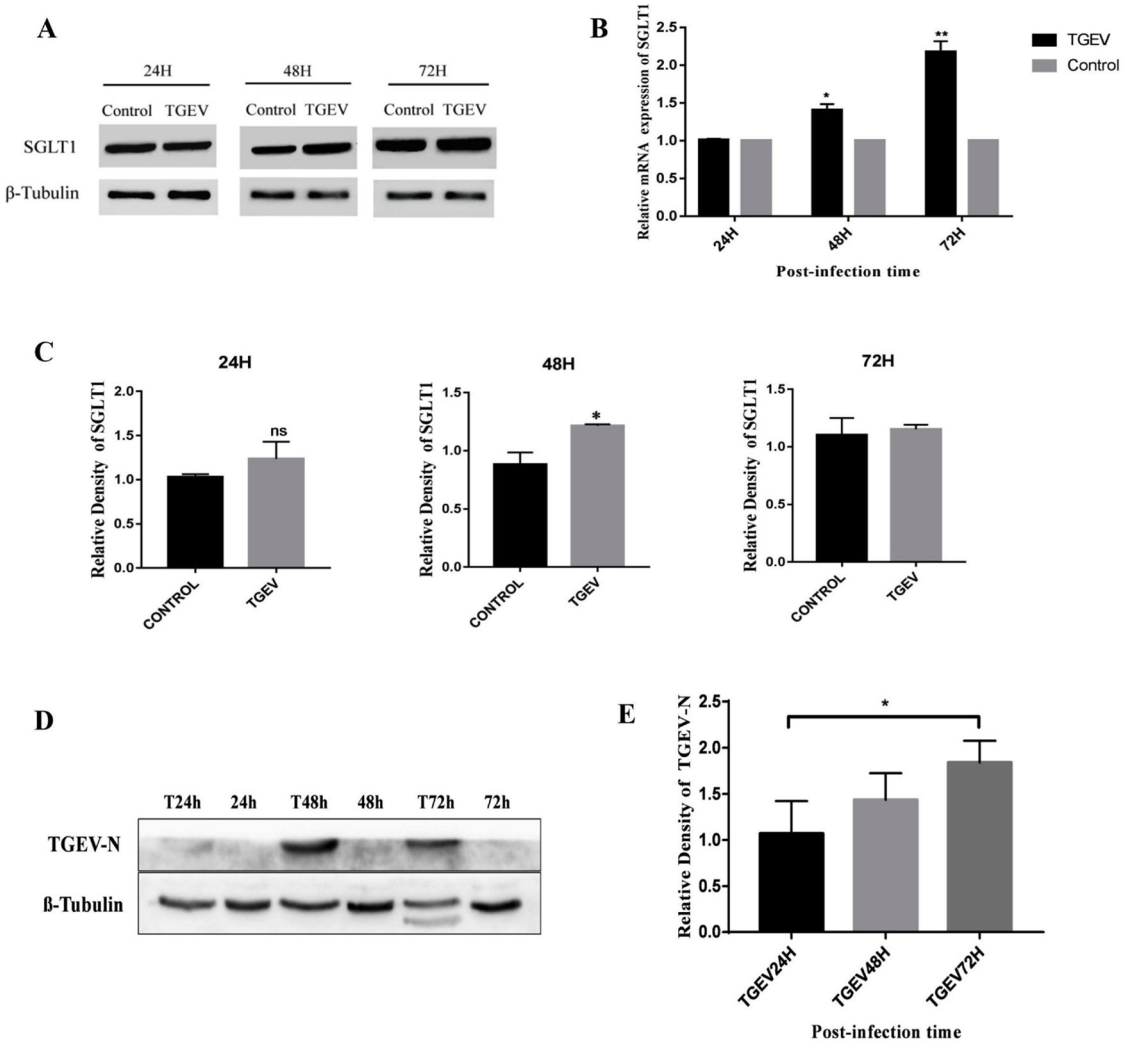

Fig. 2. (A-B) The protein expression levels of SGLT1 was determined by western blot analysis and Grayscale analysis of SGLT1 relative abundance changes. (C) SGLT1 mRNA expression levels were measured by qRT-PCR and normalized to that of the β-Actin gene. *0.01 < p < 0.05, **p < 0.01, ns represent no significant. All experiments were performed separately three times. (D) IPEC-J2 cells infected TGEV Miller (MOI = 0.1) for 24 h, 48 h, 72 h at 37 °C and TGEV-N protein expression were analyzed by western-blot. (E) Grayscale analysis of the TGEV-N.

3.4. Inhibition of SGLT1 promotes Na^+ absorption in TGEV-infected cells

To further investigate the effect of SGLT1 on sodium ion uptake following TGEV infection, we detected the intracellular and extracellular sodium ion concentration following siRNA b transfection using Flame Atomic Absorption Spectrometry. As shown in Fig. 7A, these results indicate that the intracellular Na^+ concentration of IPEC-J2 cells was extremely significantly increased following treatment with the SGLT1 inhibitor, Phlorizin, during TGEV infection. In contrast, the extracellular Na^+ concentration was reduced (Fig. 7B). To further explore the effect of SGLT1 inhibition by the treatment of cells with Phlorizin on sodium absorption mediated by NHE3, we detected NHE3 activity using the pH sensitive dye, BCECF-AM. The results suggest that NHE3 activity was significantly enhanced compared with the TGEV-infection group (Fig. 7C). Thus, we considered that the inhibition of SGLT1 could adjust the function of Na^+ absorption in IPEC-J2 cells during TGEV infection.

4. Discussion

Understanding how viruses induce diarrhea is essential to the development of more effective therapies, which is particularly important with a pathogen like coronavirus. Several previous studies have found that diarrhea is associated with NHE expression and activity. For instance, congenital sodium diarrhea (CSD) is a rare autosomal recessive diarrheal disorder with symptoms characterized by the secretion of a large volume of persistent high Na^+ diarrhea, which is considered to be related to the lack of NHE3 protein expression in vivo (Holmberg and Perheentupa, 1985; Booth et al., 1985; Janecke et al., 2016). Inflammatory bowel disease (IBD) consists of a group of chronic inflammatory diseases, the mechanisms of which involve changes in the intestinal movement and abnormal epithelial ion transport (i.e., Na^+ absorption defects in the colonic mucosa) (Clayburgh et al., 2006). One of the significant components of altered electrolyte flux in infectious diarrhea is a reduction in Na^+ absorption via impaired NHE activity, which is shown in mouse models of infection with *Salmonella typhimurium* and *Campylobacter jejuni* (Khurana et al., 1991; Kanwar et al., 2010).

However, less is known about the role of NHE in diarrhea during viral gastroenteritis. Astroviral infections have been suggested to lead to decreased levels of NHE3 in the insoluble protein fraction of enterocytes, and previous studies have shown that TGEV infection can affect changes in the both the intracellular and extracellular concentration of sodium ions in intestinal epithelial cells (Nighot et al., 2010). In our study, we found that TGEV infection could reduce the level of NHE3 protein expression on the epithelial membrane, and

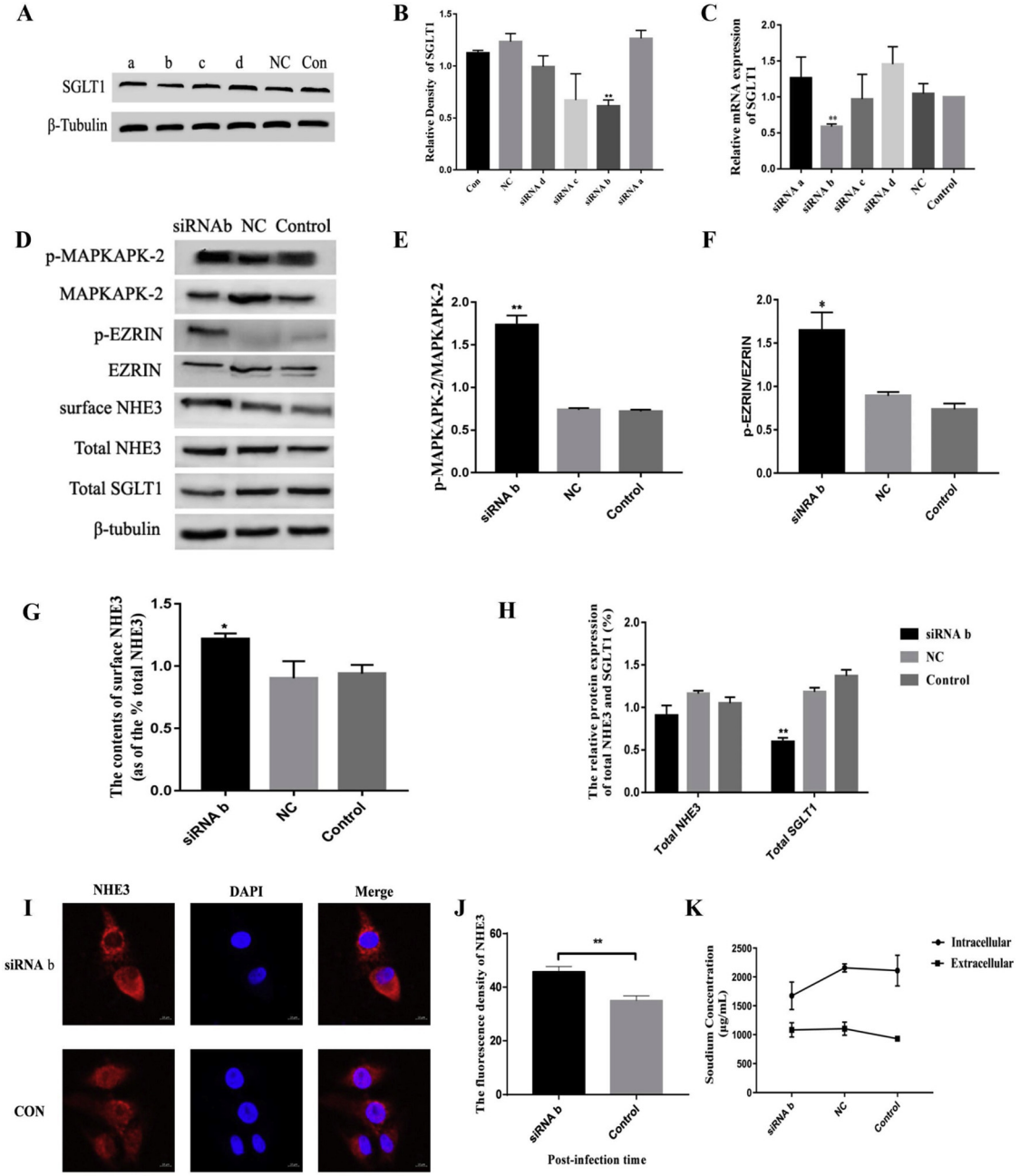

Fig. 3. NHE3 translocation was increased via down-regulation expression of SGLT1 by transfection with siRNA. (A) Western-blot analysis of the expression levels of SGLT1 after IPEC-J2 cells transfection with four siRNAs for 48 h, respectively. a represent siRNA a, b represent siRNA b, c represent siRNA c, d represent siRNA d, and NC represent empty retrovirous. (B) Grayscale analysis of the SGLT1 protein expression levels. (C) Further analysis of interference efficiency by detection of SGLT1 mRNA level using qRT-PCR. (D) Knockdown of SGLT expression by transfection siRNA b, then the expression of p-MAPKAPK-2, MAPKAPK-2, p-EARIN, EZRIN, the surface NHE3, Total NHE3, SGLT1 and β-tubulin protein were analyzed by western-blot. (E-H) Grayscale analysis of the changes in p-MAPKAPK-2/ MAPKAPK-2, p-EARIN / EZRIN, the contents of surface NHE3, toal NHE3/β-tubulin and SGLT1 level. (I)The stable expression of the siRNAb IPEC-J2 and control IPEC-J2 were seed in 24-well, then immunofluorescence as described under "Experimental Procedures". The surface NHE3 protein expression were analyzed by Image-Pro Plus 6.0. (J) fluorescence intensity of surface NHE3. (K) Intra and extracellular Na + concentration in cells transfection with siRNAb for 48 h. Each experiment was performed in triplicate. *$0.01 < p < 0.05$, **$p < 0.01$, ns represent no significant.

weakened its sodium hydrogen exchange activity, whereas the level of NHE3 mRNA was continuously increased. Thus, we concluded that the weakened the power of sodium-hydrogen exchange after TGEV infection are associated with changes in the NHE3 protein content on the cell plasma membrane, independent of transcriptional levels.

NHE3 is one of nine isoforms of the mammalian Na^+/H^+ exchanger (NHE) gene family, which is continually trafficked between the plasma membrane and intracellular organelles, and only its distribution on the plasma membrane is indicative of sodium hydrogen exchange activity (Donowitz and Li, 2007). The mechanism by which NHE3 activity is regulated is extremely complex, among which acute regulation is the most important mode of activity that includes changes in the turnover number and trafficking; the latter of which involves several regulatory proteins. Previous studies have shown that SGLT1 activation by D-glucose can initiate a linear signaling pathway that includes early activation of p38 mitogen-activated protein (MAP) kinase, followed by activation of MAP kinase activated kinase 2 (MAPK)/APK-2, phosphatidylinositol 3-kinase (PI3-K), Akt2, and Ezrin, which lead to

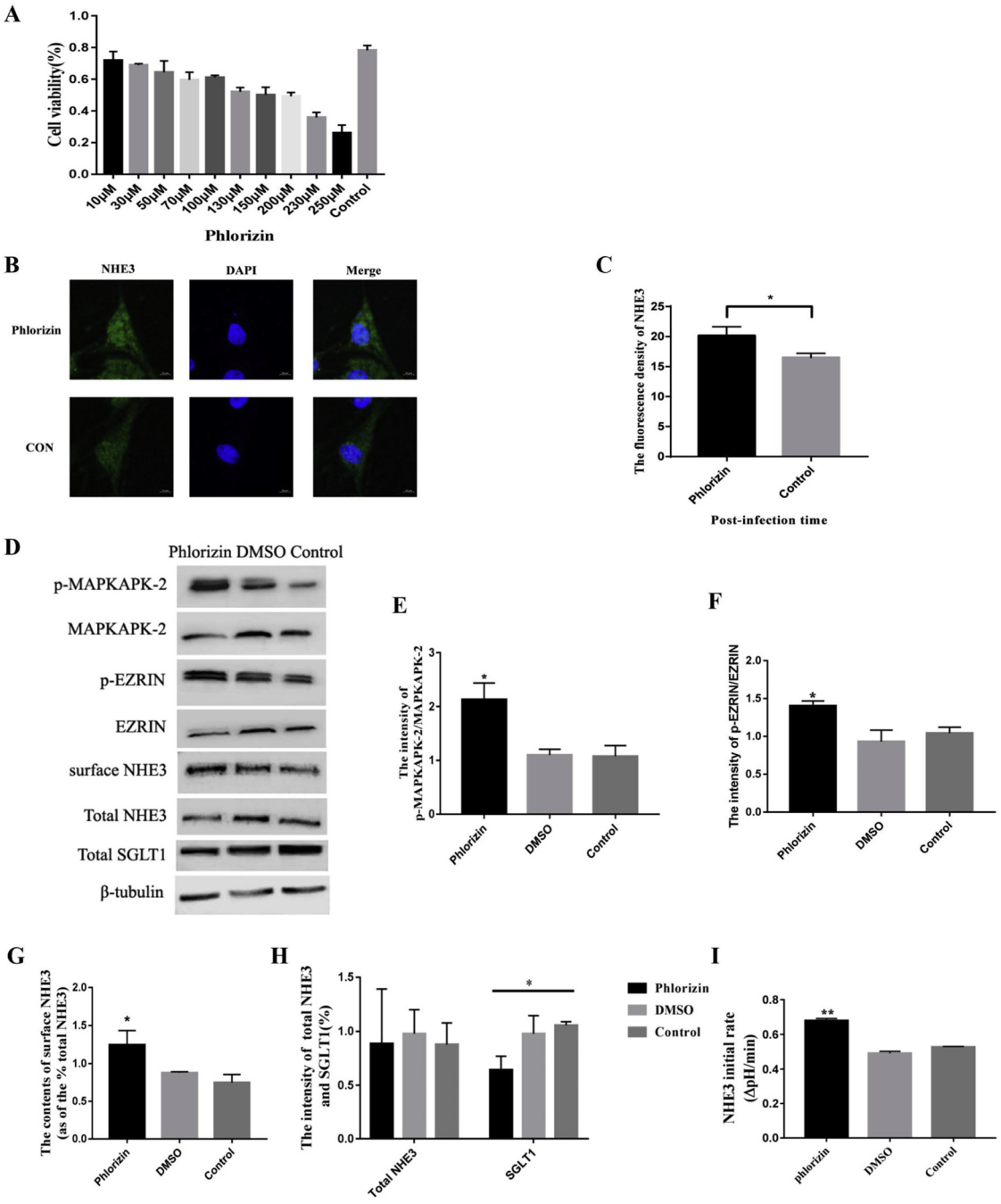

Fig. 4. Effect of inhibition of SGLT1 by treatment with Phlorizin inhibitor on the activity and translocation of NHE3. (A) MTT detection of cell viability after treatment with Phlorizin at different concentrations in IPEC-J2 cells. (B) Inhibition of SGLT1 expression by treatment with 200μM Phlorizin for 15 min, then immunofluorescence as described under "Experimental Procedures". The surface NHE3 protein expression was analyzed by Image-Pro Plus 6.0. (C) Fluorescence intensity of surface NHE3. (D) inhibition of SGLT1 expression by treatment with 200μM Phlorizin for 15 min, then the expression of p-MAPKAPK-2, MAPKAPK-2, p-EARIN, EZRIN, the surface NHE3, Total NHE3, SGLT1 and β-tubulin protein were analyzed by western-blot. (E-K) Grayscale analysis of the changes in p- MAPKAPK-2/ MAPKAPK-2,p- EARIN / EZRIN, the contents of surface NHE3, toal NHE3/β-tubulin and SGLT1 level. (L) The activity of NHE3 in cells treatment with 200μM Phlorizin for 15 min, and samples were measured using the pH sensitive dye BCECF-AM. Each experiment was performed in triplicate. *$0.01 < p < 0.05$, **$p < 0.01$.

NHE3 translocation to stimulate NHE3 activity (Cha and Donowitz, 2008). Moreover, a co-transport relationship exists between SGLT1 and NHE3 under physiological conditions (Coon et al., 2011). In the present study, we found that SGLT1 inhibition via siRNA transfection and treatment with Phlorizin could up-regulate the expression of p-MAPKAPK-2 and p-Ezrin in the p38MAPK/Akt2 pathway and increase the translocation of NHE3. In addition, there was a corresponding enhancement of sodium hydrogen exchange. As mentioned in the introduction, SGLT1 is also involved in Na^+ absorption; thus, there were no significant changes in the intracellular and extracellular concentration of Na^+ compared with the control groups after SGLT1 was inhibited by transfection with siRNA b. In conclusion, these results suggest that the inhibition of the SGLT1 expression promoted NHE3 translocation and exchange activity under physiological conditions.

TGEV infection has been shown to increase the level of SGLT protein expression at 48 h, which was consistent with previous reports by Dai

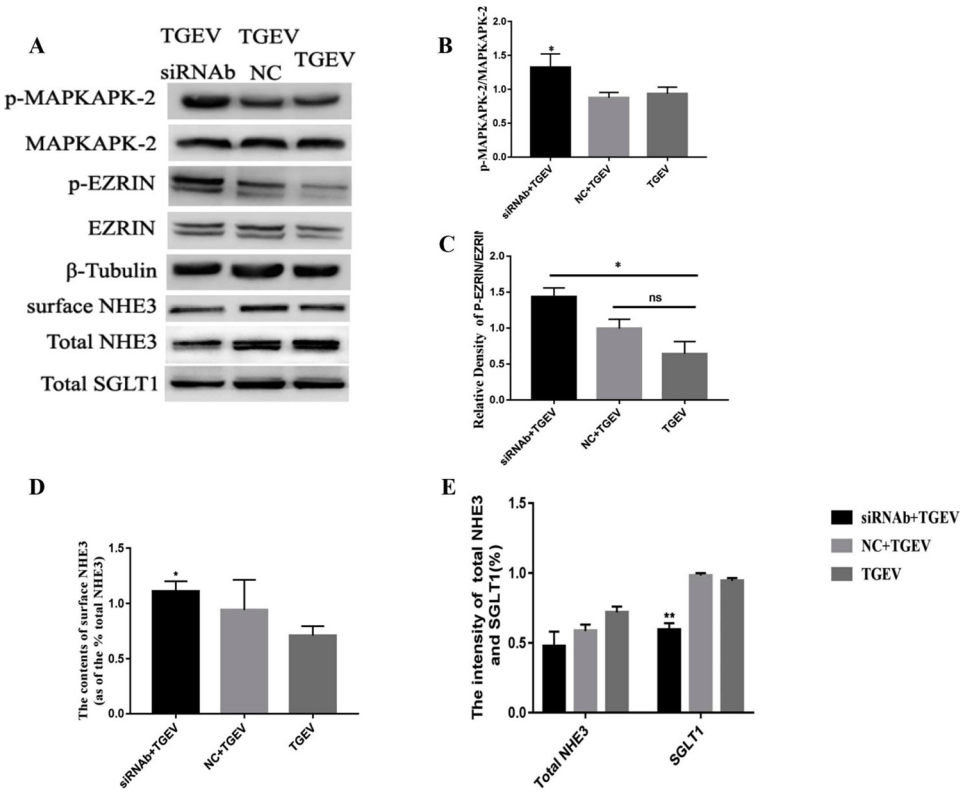

Fig. 5. TGEV regulated the surface NHE3 protein contents via SGLT1-mediated p38MAPK/AKt2 pathway. (A) IPEC-J2 infected TGEV for 48 h after Knockdown of SGLT1 expression by transfection siRNA b, then the expression of p-MAPKAPK-2, MAPKAPK-2, p-EARIN, EZRIN, the surface NHE3, Total NHE3, SGLT1 and β-tubulin protein were analyzed by western-blot. (B-E) Grayscale analysis of the changes in p-MAPKAPK-2/ MAPKAPK-2, p-EARIN / EZRIN, the contents of surface NHE3, toal NHE3/β-tubulin and SGLT1 level, Each experiment was performed in triplicate. *0.01 < p < 0.05, **p < 0.01, ns represent no significant.

et al. (Dai et al., 2016). Moreover, in Fig. 2D at 72 h post-TGEV infection, a smaller fragment of beta-Tubulin was detected, suggesting that it might be cleaved by a viral or host proteinase(s) at later stages of TGEV infection. At the same time, our previous research results showed that TGEV infection could reduce the level of surface NHE3 protein expression. Thus, we hypothesized that TGEV might regulate NHE3 trafficking by affecting the SGLT1-mediated activation of the P38MAPK/Akt2 pathway.

Therefore, the cells were transfected with SGLT1-siRNA b and treated with Phlorizin to inhibit the expression of SGLT1, followed by

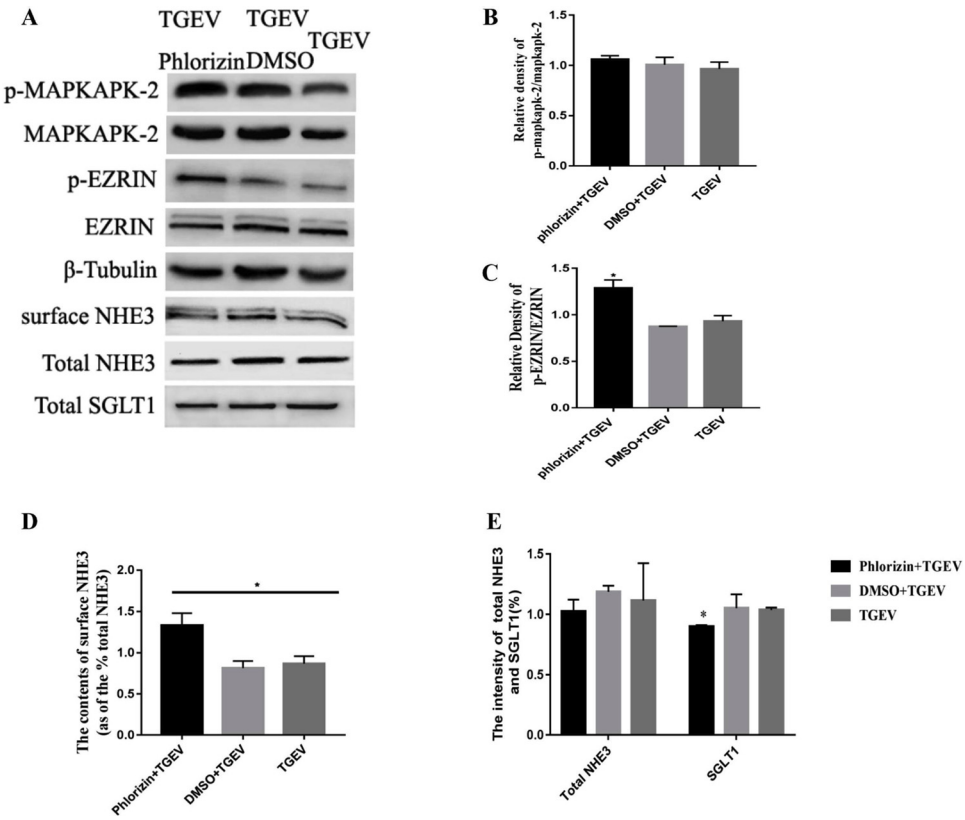

Fig. 6. Effect of inhibition of SGLT1 by treatment with Phlorizin inhibitor on the activity and translocation of NHE3. (A) IPEC-J2 infected TGEV for 48 h after inhibition of SGLT1 expression by treatment with 200μM Phlorizin, then the expression of p-MAPKAPK-2, MAPKAPK-2, p-EARIN, EZRIN, the surface NHE3, Total NHE3, SGLT1 and β-tubulin protein were analyzed by western-blot. (B-E) Grayscale analysis of the changes in p-MAPKAPK-2/ MAPKAPK-2, p- EARIN / EZRIN, the contents of surface NHE3, toal NHE3/β-tubulin and SGLT1 level, Each experiment was performed in triplicate. *0.01 < p < 0.05.

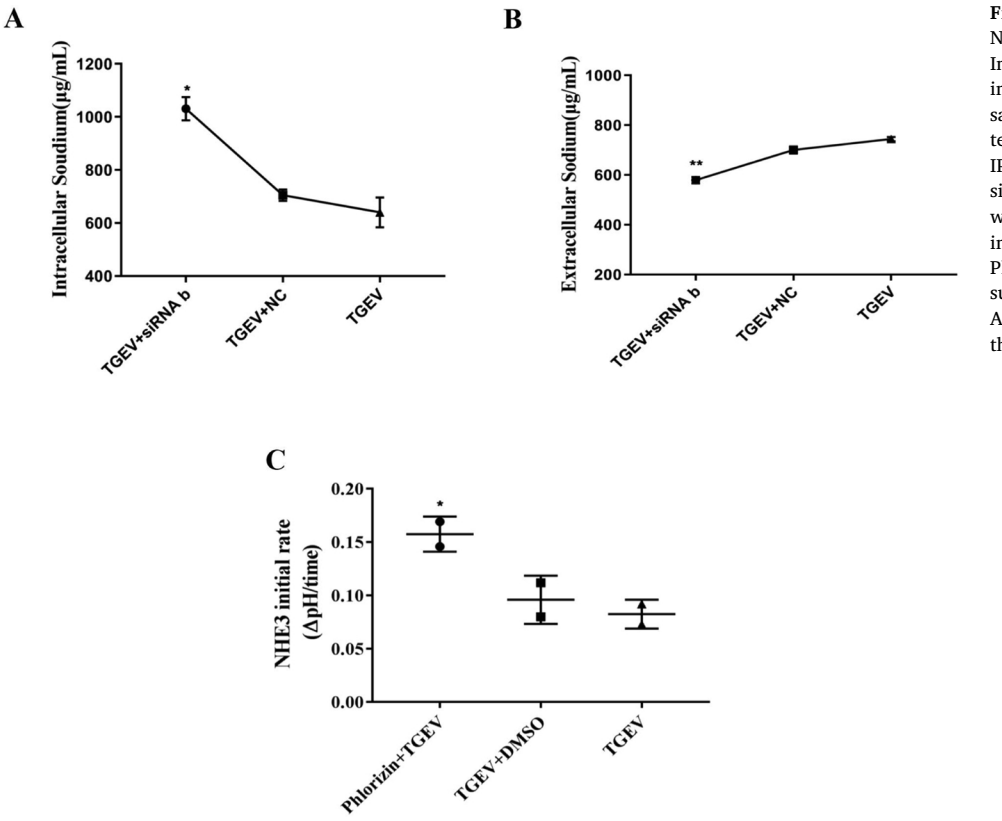

Fig. 7. Effect of inhibition of SGLT1 on the Na + absorption in TGEV-infected cells. (A) Intracellular Na + concentration in IPEC-J2 infection TGEV after transfection with siRNA, samples collected from the cell lysate were tested. (B) Extracellular Na + concentration in IPEC-J2 infection TGEV after transfection with siRNA, samples from the cell culture medium were tested. (C) The activity of NHE3 in TGEV infection after cells treatment with 200μM Phlorizin for 15 min, and samples were measured using the pH sensitive dye BCECF-AM. All experiments were performed separately three times, *0.01 < p < 0.05, **p < 0.01.

an incubation with TGEV. We then found that the level of p-MAPKAPK-2 and p-EZRIN protein expression were both reduced following TGEV infection after transfection with SGLT1-siRNA b, and enhanced NHE3 trafficking and the power of Na^+ absorption. TGEV infection had no significant effect on the level of p-MAPKAPAK-2 protein expression after IPEC-J2 cells were treated with Phlorizin; however, the surface NHE3 protein content was still increased, and the activity of Na^+ absorption was enhanced. It has been established that since Phlorizin is a non-selective SGLT inhibitor, when applied to a target, it may affect the expression and activity of other proteins. Therefore, while there was no change in the level of phosphorylation of the upstream proteins, the downstream phosphoric acid levels remained up-regulated. We suspect that there may be other signaling pathways involved in the common regulation of EZRIN-mediated NHE3 translocation. These data suggest that TGEV infection may weaken NHE3 activity due to a reduction of surface NHE3 protein content through SGLT1-mediated activation of the P38MAPK/Akt2 signaling pathway, and this may provide a new strategy for treating diarrhea in infected piglets.

CRediT authorship contribution statement

Yang Yang: Conceptualization, Methodology, Investigation, Formal analysis, Resources, Writing - review & editing, Writing - original draft, Writing - review & editing. **Qiuhan Yu:** Formal analysis, Resources, Writing - review & editing, Writing - original draft, Writing - review & editing. **Han Song:** Investigation, Conceptualization, Methodology, Supervision, Project administration, Funding acquisition. **Ling Ran:** Investigation, Conceptualization, Methodology, Supervision, Project administration, Funding acquisition. **Kai Wang:** Investigation, Conceptualization, Methodology, Supervision, Project administration, Funding acquisition. **Luyi Xie:** Investigation, Conceptualization, Methodology, Supervision, Project administration, Funding acquisition. **Shilei Huang:** Investigation, Conceptualization, Supervision. **Zheng Niu:** Investigation, Conceptualization, Methodology, Supervision, Project administration, Funding acquisition. **Yilin Zhang:** Formal analysis, Resources, Writing - review & editing. **Zifei Kan:** Investigation, Conceptualization, Methodology, Supervision, Project administration, Funding acquisition. **Tao Yan:** Investigation, Conceptualization, Methodology, Supervision, Project administration, Funding acquisition. **Zhenhui Song:** Conceptualization, Methodology, Investigation.

Declaration of Competing Interest

The authors declare that there are no conflicts of interest.

Acknowledgments

The authors gratefully acknowledge each member of the research team for supporting this project, and other veterinary medicine students from Southwest University for their valuable suggestions and assistance. This work was supported by the Fundamental Research Funds for the Central Universities (XDJK2020RC001), and Venture & Innovation Support Program for Chongqing Overseas Returnees (cx2019097).

References

Booth, I.W., Murer, H., Stange, G., Fenton, T.R., Milla, P.J., 1985. Defective jejunal brush-border na + /h + exchange: a cause of congenital secretory diarrhoea. Lancet 325 (8437), 1066–1069.

Brett, C.L., 2005. The yeast endosomal Na + (K +)/H + exchanger Nhx1 regulates cellular pH to control vesicle trafficking[J]. Mol. Biol. Cell 16 (3), 1396–1405.

Butler, D.G., Gali, D.G., Kelly, M.H., Hamilton, J.R., 1974. Transmissible gastroenteritis mechanisms responsible for diarrhea in an acute viral enteritis in piglets. J. Clin. Invest. 53 (5), 1335–1342.

Cha, B., Donowitz, M., 2008. The epithelial brush border na + /h + exchanger nhe3 associates with the actin cytoskeleton by binding to ezrin directly and via pdz domain-containing na + /h + exchanger regulatory factor (nherf) proteins. Clin. Exp. Pharmacol. Physiol. 35 (8), 863–871.

Chow, Chung-Wai, Khurana, Seema, Woodside, Michael, Grinstein, Sergio, Orlowski, John, 1999. The epithelial Na + /H +, exchanger, NHE3, is internalized through a clathrin-mediated pathway *[j]. J. Biol. Chem. 274.

Clayburgh, Daniel R., Yang-Xin, Fu, Turner, Jerrold R., 2006. Coordinated Epithelial NHE3 Inhibition and Barrier Dysfunction Are Required for TNF- Mediated Diarrhea in Vivo.
Coon, S., Kekuda, R., Saha, P., Sundaram, U., 2011. Reciprocal regulation of the primary sodium absorptive pathways in rat intestinal epithelial cells. Am. J. Physiol., Cell Physiol. 300 (3), 496–505.
D'Souza, S., Garcia-Cabado, A., Yu, F., Teter, K., Lukacs, G., Skorecki, K., et al., 1998. The epithelial sodium-hydrogen antiporter na+/h+ exchanger 3 accumulates and is functional in recycling endosomes. J. Biol. Chem. 273 (4), 2035–2043.
Dai, L., Hu, W.W., Xia, L., Xia, M., Yang, Q., 2016. Transmissible gastroenteritis virus infection enhances sglt1 and glut2 expression to increase glucose uptake - fig 2. PLoS One 11 (11), e0165585.
Donowitz, M., Li, X., 2007. Regulatory binding partners and complexes of nhe3. Physiol. Rev. 87 (3), 825–872.
Dynia, D.W., Steinmetz, A.G., Kocinsky, H.S., 2010. Nhe3 function and phosphorylation are regulated by a calyculin a-sensitive phosphatase. Ajp Ren. Physiol. 298 (3), F745–F753.
Field, M., 2003. Intestinal ion transport and the pathophysiology of diarrhea. J. Clin. Invest. 111 (7), 931–943.
Holmberg, C., Perheentupa, J., 1985. Congenital na+ diarrhea: a new type of secretory diarrhea. J. Pediatr. 106 (1), 56–61.
Janecke, A.R., Heinz-Erian, P., Müller, T., 2016. Congenital sodium diarrhea: a form of intractable diarrhea, with a link to inflammatory bowel disease. J. Pediatr. Gastroenterol. Nutr. 63 (2), 170.
Janecki, A.J., 2000. Basic fibroblast growth factor stimulates surface expression and activity of na+/h+ exchanger nhe3 via mechanism involving phosphatidylinositol 3-kinase. J. Biol. Chem. 275 (11), 8133–8142.
Kanwar, R.K., Ganguly, N.K., Kanwar, J.R., Kumar, L., Walia, B.N.S., 2010. Impairment of na+,k+-atpase activity following enterotoxigenic campylobacter jejuni infection: changes in na+, cl− and 3-o-methyl-d-glucose transport in vitro, in rat ileum. FEMS Microbiol. Lett. 124 (3), 381–385.
Katsuda, K., Kohmoto, M., Kawashima, K., Tsunemitsu, H., 2006. Frequency of enteropathogen detection in suckling and weaned pigs with diarrhea in japan. J. Vet. Diagn. Investigation Official Publ. Am. Assoc.Vet. Lab. Diagnosticians Inc 18 (4), 350.
Kelly, M., Butler, D.G., Hamilton, J.R., 1972. Transmissible gastroenteritis in piglets: a model of infantile viral diarrhea. J. Pediatr. 80 (6), 925–931.
Khurana, S., Ganguly, N.K., Khullar, M., Panigrahi, D., Walia, B.N.S., 1991. Studies on the mechanism of salmonella typhimurium enterotoxin-induced diarrhoea. Biochimica et Biophysica Acta (BBA) - Molecular Basis of Disease 1097 (3), 171–176.
Lawhorn, D.B., 2007. Diarrheal Disease in Show Swine. Texas A M University.
Leopoldt, D., Meyer, U., 1978. [Transmissible gastroenteritis of swine as a model for infectious diarrhea]. Archiv Für Experimentelle Veterinärmedizin 32 (3), 417.
Murtazina, R., Kovbasnjuk, O., Donowitz, M., Li, X., 2006. Na + /h +, exchanger nhe3 activity and trafficking are lipid raft-dependent *. J. Biol. Chem. 281.
Nighot, P.K., Moeser, A., Ali, R.A., Blikslager, A.T., Koci, M.D., 2010. Astrovirus infection induces sodium malabsorption and redistributes sodium hydrogen exchanger expression. Virology 401 (2), 146–154.
Schultheis, P.J., Clarke, L.L., Meneton, P., Miller, M.L., Shull, G.E., 1998. Renal and intestinal absorptive defects in mice lacking the nhe3 na+/h+ exchanger. Nat. Genet. 19 (3), 282–285.
Tajima, M., 1970. Morphology of transmissible gastroenteritis virus of pigs. Arch. Fã¼r Die Gesamte Virusforsch. 29 (1), 105–108.
Wright, E.M., Loo, D.D.F., Hirayama, B.A., Turk, E., 2004. Surprising versatility of na+-glucose cotransporters: slc5. Physiology 19 (6), 370–376.
Xia, L., Yang, Y., Wang, J., Jing, Y., Yang, Q., 2018. Impact of tgev infection on the pig small intestine. Virol. J. 15 (1), 102.
Xu, H., Ghishan, F.K., Kiela, P.R., 2018. SLC9 Gene Family: Function, Expression, and Regulation. Comprehensive Physiology. American Cancer Society.
Yang, Z., Ran, L., Yuan, P., Yang, Y., Wang, K., Xie, L., et al., 2018. EGFR as a negative regulatory protein adjusts the activity and mobility of nhe3 in the cell membrane of ipec-j2 cells with tgev infection. Front. Microbiol. 9.
Zhang, Zhi-Bo, Han, Xue-Feng, Tan, Zhi-Liang, Xiao, Wen-Jun, 2012. Progress in understanding the relationship between diarrhea and intestinal ion transport. China Acdamical journal Electronic Publishing House 20 (9), 743–748 2012.